Int J Fract (2013) 184:171–183
DOI 10.1007/s10704-013-9858-8

ORIGINAL PAPER

A solution to the parameter-identification conundrum: multi-scale interaction potentials

J. G. M. van Mier

Received: 30 October 2012 / Accepted: 19 March 2013 / Published online: 5 June 2013

Abstract Softening is a structural property, not a material property. Any material will show softening, but in this paper the focus is primarily on cement and concrete, which show this property very clearly owing to their coarse heterogeneity (relative to common laboratory-scale specimen sizes). A new model approach is presented, based on pair-potentials describing the interaction between two neighbouring particles at any desired size/scale level. Because of the resemblance with a particle model an equivalent lattice can be constructed. The pair-potential is then the behavioral law of a single lattice element. This relation between force and displacement depends on the size of the considered lattice element as well as on the rotational stiffness at the nodes, which not only depends on the flexibility of the global lattice to which the element is connected but also on the flexural stiffness of the considered element itself. The potential $F - r$ relation is a structural property that can be directly measured in physical experiments, thereby solving size effects and boundary effects.

Keywords Concrete · Fracture · Model parameters · Interaction potentials ($F - \delta$) · Size effect · Asymptotic behaviour

J. G. M. van Mier
Swiss Federal Institute of Technology(ETH Zurich),
8093 Zurich, Switzerland
e-mail:jvanmier@ethz.ch

1 Introduction

A reliable model for fracture of concrete is helpful for the design of strong and flexible structures that can withstand a variety of complex loadings. Two properties of concrete are of great importance when considering fracture. First of all, the material has a very low tensile strength, much lower than its compressive resistance. The imbalance between tensile and compressive strength becomes even larger when high (compressive) strength concrete is applied. Also in the case of confined compression the relative difference increases. The second, for fracture very important characteristic of concrete is its rough heterogeneity. The heterogeneity is a consequence of economics: reducing the price of concrete through the addition of relatively cheap sand and gravel to the more expensive binder (Portland) cement is common practice. Not only the costs of concrete decrease, the properties improve in comparison to the properties of pure hardened Portland cement, in particular the cement's brittleness is partly overcome. Models for concrete for structural applications are generally based on continuum mechanics. This 400-year old methodology is based on the assumption that material properties can be described using stress and strain as state variables, or stated differently, the mechanical behaviour of the material can be described by means of average properties. Central to developing a sound continuum-based theory is, not surprisingly, the so called Representative Volume Element (RVE), i.e. the smallest material volume needed to define the

average properties of the considered material. Conventional wisdom learns that the RVE should at least be a factor 3 to 5 larger than the largest heterogeneity found in the material. For concrete, but also other materials, the size of the grains is considered when defining the RVE. From a series of uniaxial tensile tests on specimens of varying size we concluded that the RVE should be larger than at least 8 times the maximum aggregate size, see Van Vliet and Van Mier (2000). This conclusion was based on the observation that beyond this threshold the scatter in the experiments decreases and becomes more-or-less constant. Small specimens, or rather, small structures show clearly the effect of heterogeneity. The increase of scatter below the aforementioned threshold increases as one single aggregate may be responsible for the structure's behaviour. Next to this, what we will call 'RVE-based-on-fixed-material-structure', clearly the size of nucleating and actively growing cracks must be considered. If a crack increases to a size of the same order of magnitude as the characteristic specimen size, boundary condition effects and geometry-related effects cannot be ignored any longer. In concrete cracks are not only caused by mechanical loading, but environmental conditions may have a profound influence as well. Differential temperature distributions during the hydration of cement (when concrete hardens) and/or differential moisture content in various part of a structure lead to eigen-stresses and with that, if the strength threshold is exceeded to crack nucleation and growth.

Owing to the coarse heterogeneity of concrete severe stress concentrations are present in the material when external load is applied. The stress-concentrations are the results from E-mismatch between the various material phases in the composites and the material's porosity. An important factor leading to crack growth in concrete at moderate external loading levels is the low tensile strength of the interfacial transition zone (ITZ) between matrix and aggregates. It is noted that when we would scale-down the specimen/structure size below the aggregate size, and zoom-in on a volume of cement matrix, the same observations can be made. Compared to the cement structure small sand grains will be relatively coarse and cause stress-concentrations. Going further down in scale will bring us to the scale of the cement binder. Here we will find un-hydrated cement, and the hydration products, which again can be seen as aggregates (now the un-hydrated cement kernels) embedded in a matrix with a clear smaller material structure (the structure of hydrated cement is found at nm-size/scale).

Thus, obviously, concrete and also cement are highly heterogeneous at various size/scale levels. It would be tempting to address the heterogeneity of concrete (and cement) via a fractal analysis, but it appears that 'jumps' are made along the dimensional scale, which would demand for a multi-fractal approach. We will not discuss these matters further, but rather suggest a different solution that will incorporate heterogeneity at any size/scale level implicitly. The proposed solution is based on a lattice model. Lattice models have been suggested as a tool for analyzing fracture of disordered materials in the last two decades of the past century, see for instance Roux and Guyon (1985), Termonia and Meakin (1986) and Herrmann et al. (1989), among many others. Since 1990 we have applied lattice-type models for simulating fracture of concrete, which has shown to be a valuable tool for obtaining a better understanding of fracture, be it that the approach is most fruitful when at the same time relevant experiments are carried out; see for instance Schlangen and Van Mier (1992) and Lilliu and Van Mier (2003) for 2D- and 3D-versions of the 'Delft' lattice model. Quite essential in our approach has been to incorporate the structure of concrete (or cement) directly into the model. Various methods are available to do so; the interested reader is referred to Van Mier (2012) for an overview. In a lattice model the material is modeled as a regular or irregular network of linear elements. For fracture it appears that the most realistic results are obtained if beam elements are used. By means of a finite element program forces and deformations in the network are calculated, and given a fracture criterion it can be decided which of the elements will break. Fracture is simulated by removing in each load-step just one element, re-calculating the stress-redistributions after removal, after which the next critical element is determined and removed. The disadvantage of this rather coarse way of simulating fracture is that the calculated load-displacement curves are generally too brittle. This can be repaired by including a softening stress-crack opening relation for the lattice elements as proposed by Ince et al. (2003). The obvious disadvantage is that not only the computation becomes more elaborate but also the softening stress-crack opening is in principle 'un-determined. The main advantage of our lattice approach based on element removal is that it is simple and transparent. No complicated iterative

procedures are needed, which is quite essential if the model is used in combination with experiments. The goal is getting a better understanding of fracture mechanisms in disordered materials like concrete; it is certainly not an attempt to develop a simulation model that can be fitted as closely as possible to experimental data. Up till now always the decision to fracture an element was based on a simple 'stress-criterion', i.e. when stresses in a lattice element would exceed a prescribed maximum stress (e.g. normal stress, flexural stress, etc.) the element would fail instantaneously (elastic-purely brittle). This implies that still continuum beam theory is used to decide whether an element will fail or not. In view of the statements regarding the RVE this is quite extraordinary (and probably not correct) since in the aforementioned lattice models the size of a lattice element is in the same order as the material's heterogeneity, for instance in concrete usually the lattice element length is selected 3 to 4 times smaller than the smallest aggregate particle incorporated in the material structure. Clearly there is reason to look at these matters in a different way, which is precisely what we will do in this paper.

The organization of the paper is as follows. In Sect. 2 we will argue that softening is a structural property, not a material property. This distinction is quite essential since it will be necessary to deviate from cohesive fracture models. In Sect. 3 we will show that the consequence of softening as a structural property, multi-scale approaches are deemed to fail. Rather an approach called 'up-scaling' from a pre-defined smallest size/scale level seems a more realistic option, which is then worked out in Sect. 4 for fracture of concrete. The softening relation needed in the 'structural lattice' debated in Sect. 4 is no longer expressed in terms of σ and δ, but rather in F and δ, and must be regarded as the structural property of a lattice element. A consequence is that the sought relationship between F and δ depends on the structural boundary conditions (fixed or pinned support; more general, the rotational stiffness k_r of the supports) and on the size of the lattice element, viz. a structural property. This is precisely what can be measured routinely in basic experiments in concrete technology, namely the uniaxial tensile properties and the (confined) compressive behaviour. A further advantage of using a 'structural' lattice model is that very likely compressive fracture can be captured in a lattice model as well. Buckling of lattice elements can be considered and can be included in the model in a relatively simple and straightforward manner. Again here we find the significant influence of boundary conditions and element slenderness (geometry), which is now incorporated directly into the model. Finally, in Sect. 5 methods are suggested that can be used to validate the new model approach. Without that the model would be incomplete as so many models are today.

2 What can be measured directly in fracture experiments?

In popular cohesive models for concrete the crack-tip closing stress is modeled according to the outcome of a uniaxial tension test between fixed (non-rotating) loading platen. This is what the fictitious crack model developers tell us; see Hillerborg et al. (1976). Since the early 1980s there have been numerous efforts to establish a standard tension or bending test that would help quantifying the properties needed in the fictitious crack model. What all experiments tell, however, is that none of the required properties for the fictitious crack model are true material properties. These parameters are the tensile strength f_t, the fracture energy G_f, the maximum crack opening δ_c and the shape of the softening curve $\sigma(\delta)$. In some way they all depend on specimen size, specimen geometry and boundary conditions. Drawing an equivalent to fracture under (confined) compression shows the same effects, albeit in this case specimen geometry and boundary conditions appear to be even more influential. In the case of tensile fracture researchers often revert to in-direct tests under the argument that uniaxial tension tests are too difficult. Instead seemingly simple experiments are carried out like the Brazilian splitting test or a (3-point of 4-point) bending test on prismatic beams. These latter tests require back-analysis of the results, and thus a number of assumptions are usually needed that are not always realistic. Here we focus on uniaxial tension and draw a parallel to uniaxial compression tests because both tests can deliver the data needed for the 'structural' lattice model, which is presented in Sect. 4. Observations from uniaxial tension and uniaxial compression tests lead to the following overview:

(1) When considering concrete the characteristic specimen size should be larger than 100–150 mm (i.e. 5 to 8 times the maximum aggregate size); for concretes with very large aggregates (dam concrete)

this would lead to even larger specimen sizes. Along the same lines of reasoning: for hardened cement paste the minimum required specimen size would be 500–1000 μm.

(2) In the fictitious crack model it has become common practice to model the pre-peak stress-strain curve as purely linear elastic. Experiments by Evans and Marathe (1968) indicate that already at a relatively low stress-level in the pre-peak regime microcracking starts. This is also the outcome from own experiments and simulations, see Van Mier (2009).

(3) The fictitious crack model tells us that microcracks propagate and widen in the softening regime. This is not true. Not only the experiments by Evans and Marathe (1968) lead to a different conclusion, a survey carried out by Mindess (1991) shows that the extent of a fracture process zone, commonly associated with the length of the crack-tip bridging zone, not only depends on specimen geometry but also on the accuracy of the crack detection methods used. It is also easy to show that in the softening regime a macroscopic crack dominates the behaviour of a test specimen, see Van Mier and Nooru-Mohamed (1990). These finding for uniaxial tension can easily be extended to (confined) compression; see Van Mier (2012).

(4) The specimen size has a significant influence on the tensile strength of a specimen. In general tensile strength will decrease with increasing specimen size (Fig. 1a); see for instance Van Vliet and Van Mier (2000) and Van Mier and Van Vliet (2003). Several (competing) theories describe this decrease of structural strength with specimen/structure size; see for instance Weibull (1939), Bažant (1984) and Carpinteri et al. (2003). The theory by Weibull is the only size effect approach based on sound physics. The main assumption here is that large structures have a larger probability of containing defects and hence are weaker. The other two models, sometimes dubbed 'laws' are exercises in curve-fitting. Quite important in both latter approaches is the notion of the asymptotic behaviour for small and large sizes (see Fig. 1a). Trying to validate the asymptotic behaviour in the small size range is impossible: as soon as the specimen/structure size becomes smaller than the RVE experimental scatter will become larger and a solid conclusion cannot be drawn. The RVE is estimated at $8d_a$ and indicated in Fig. 1a. The large-size asymptotic behaviour cannot be established either because the laboratory facilities will be decisive for the maximum size of a specimen/structure that can be tested. In most labs the characteristic specimen size will not exceed 2 m. A workable option would be to test larger specimens floating on water. The large-size asymptote is considered more important than the lower-size asymptote for the sole reason that such results can be used directly in structural engineering. Note that at the lower-size asymptote, below the RVE, we start testing different materials, namely the individual constituents of concrete: hardened cement paste and aggregate. In Fig. 1a conclusions about models and experiments can only be drawn in the area enclosed by the box of the diagram. Beyond these boundaries only fruitless speculation is possible; many hours have been lost at conferences in the past decade debating the best 'size effect law' on the basis of the behaviour at the extremes. It is obvious that it is impossible to discriminate between the proposed models (Bažant 1984 and Carpinteri et al. 2003) simply because it will never be possible to validate the speculations by means of physical experiment.

(5) With increasing specimen/structure size the fracture energy (i.e. the area under the post-peak softening curve) increases as shown in Fig. 1b. For large sizes ($>$ 1.6 m for 8-mm concrete) the curve seems to level of towards a horizontal asymptote. Therefore it is believed that fracture energy may be a true material property, but very large specimens are needed to make the actual measurements for a given concrete. Models based on local fracture energy g_f (for instance Duan and Hu 2004) are difficult to feed with experimental data simply because at the lower end of the size-scale measurements of fracture energy will not yield realistic values. The complete stress-deformation diagram is affected when specimen/structure size increases. Larger specimens show a more brittle behaviour; just beyond peak even snap-back behaviour may occur depending on the choice of control parameter in the closed-loop testing system (see also references mentioned in the next paragraph).

(6) It is by no means clear for which characteristic specimen size the softening diagram needed in the fictitious crack model must be determined. Obtaining a stable softening diagram is not easy if

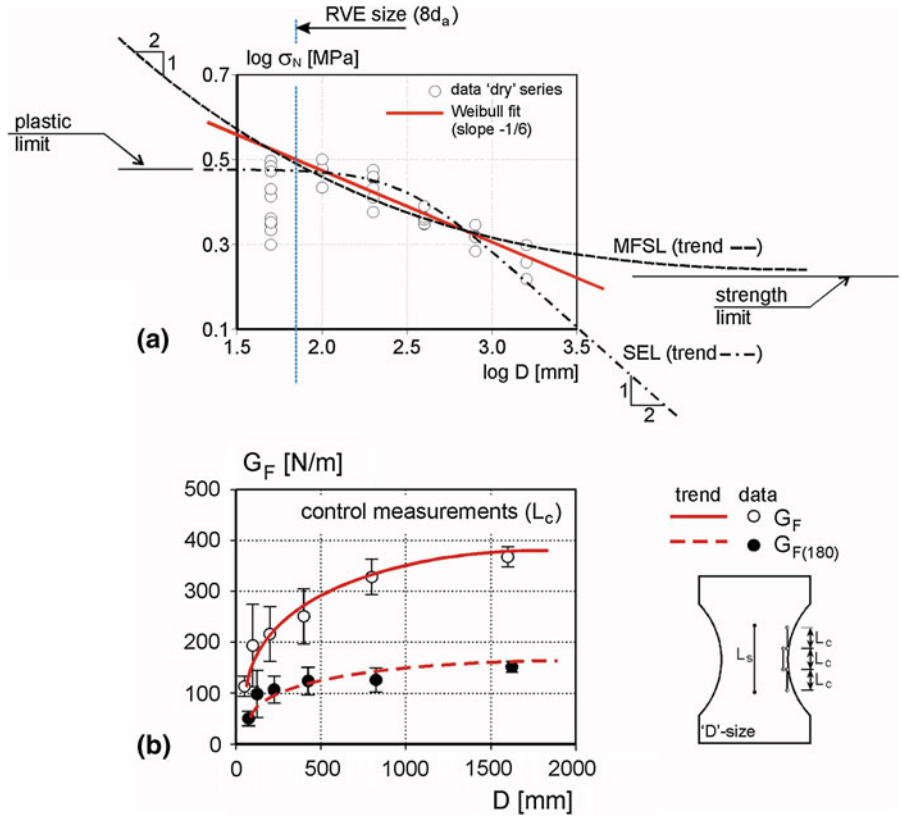

Fig. 1 Size effect on structural strength (**a**) and fracture energy (**b**) from uniaxial tensile tests on dog-bone shaped specimens. Testing below the RVE-size (taken here as $8\,d_a$, and indicated in (**a**)) is not possible due to increasing scatter. Therefore assumed asymptotic behaviour in the small size/scale regime can never be validated experimentally. The fracture energy has been calculated up till 180 μ m crack opening, denoted as $G_{F,180}$ and till full separation G_F. In the latter case measured curves were linearly extrapolated to the point where they intersected with the x-axis. Data are from Van Mier and Van Vliet (2003). The Weibull theory has been fitted to the experimental data; for SEL and MFSL only trends are shown indicating the asymptotic behaviour for small and large sizes

the right equipment is lacking, see Van Mier and Shi (2002). Considering that the fracture energy grows towards an asymptotic value for larger specimens, this might indicate that even larger specimens (2-m range) would be required than based on considering the RVE. At those larger sizes maintaining stability of crack growth in the softening regime is most difficult because often snap-back behaviour may occur. The difficulties can be overcome, however, as shown in Van Vliet and Van Mier (2000) and Van Mier and Shi (2002), but require next to the servo-hydraulic control system some additional electronics.

(7) Boundary conditions have a pronounced influence on the softening behaviour, both in tension and under (confined) compression. More specifically, in tension the rotational freedom at the nodes affects the tensile strength, the pre-peak non-linearity, the shape of the softening curve and the fracture energy. In (confined) compression, in addition to the rotational freedom of the supports the frictional restraint at the specimen-loading platen interface must be considered. In Fig. 2 three different cases are shown: fixed boundaries ($k_r = \infty$) using a slender specimen ($h/d > 2$) in Fig. 2a, pinned boundaries ($k_r = 0$) using a slender specimen in Fig. 2b and in Fig. 2c a stubby specimen ($h/d < 1$) loaded between fixed boundaries. With fixed boundaries two cracks will develop in the softening regime; restraining the rotations at the specimens ends will cause the bump in the diagram as the two cracks develop in sequence from two opposite

sides of the specimen, see Van Mier (1986). In contrast, when a slender specimen is loaded between pinned boundaries the first crack to develop is also the crack leading to complete failure of the specimen, i.e. no secondary cracking can occur. The fracture energy is markedly smaller in the second case as a direct consequence of the reduced crack area; the tensile strength is smaller under pinned boundaries in comparison to fixed boundaries; see Van Mier et al. (1995). When a stubby specimen is used instead of a slender specimen the stress-redistributions occur earlier, around peak, and results by Hordijk (1991) show that the pre-peak part of the diagram becomes more curved, the deformation at peak-load increases and the 'bump' has disappeared. The result is shown schematically in Fig. 2c. More recently, Akita et al. (2007) showed that the specimen shape has a significant effect on tensile strength as well.

(8) As a consequence of the size effect on strength and deformation, and the influence of boundary rotations it is impossible to choose the 'best' or 'most appropriate' type of experiment for determining the softening diagram of concrete in tension and with that the closing stress-profile in a cohesive fracture model. The point of view that comes closest to all results is that softening is a 'structural property', rather than a 'material property'. It is impossible to separate boundary effects from material effects in all these experiments. The main reason is that a crack with a size comparable to the specimen/structure dimensions is developing, and like in classical fracture mechanics a correction for these effects must be incorporated in any model trying to deal with the aforementioned phenomena. Thus, the behaviour measured in a uniaxial tensile test is valid only for the chosen specimen size and the applied boundary conditions. The resulting $F-\delta$ relation should be used directly in a model, as this is the only un-biased result that can be derived from an experiment. We will return to these matters in Sect. 4. It should be noted that the last remaining 'continuum state variable' in the fictitious crack model has been dropped; rather than giving results in terms of average stress over the specimens cross-section it will be an improvement to present matters directly in force and displacement, thereby also incorporating the pre-peak behaviour in the formulation. Note that this is a significant deviation from the fictitious crack model.

For compressive fracture the same situation emerges, see Van Mier (2009, 2012). Next to the chosen boundary rotations also frictional restraint between loading platen and specimen ends will affect the measurements. Higher boundary restraint results in a higher compressive strength, larger deformations at peak stress and a shallower softening branch. The interested reader is referred to my recent book for a complete overview of all factors affecting compressive fracture; see Van Mier (2012). The aforementioned effects will also be found under confined compression, provided the confinement stays below the brittle-to-ductile transition.

In conclusion to this section it can be stated that it does not make sense to continue with cohesive fracture models for concrete. The essential parameter, the $\sigma-w$ relation is not a 'material property' but must be seen as the response of the complete specimen-machine system. Softening is a 'structural property'. In Sect. 4 we

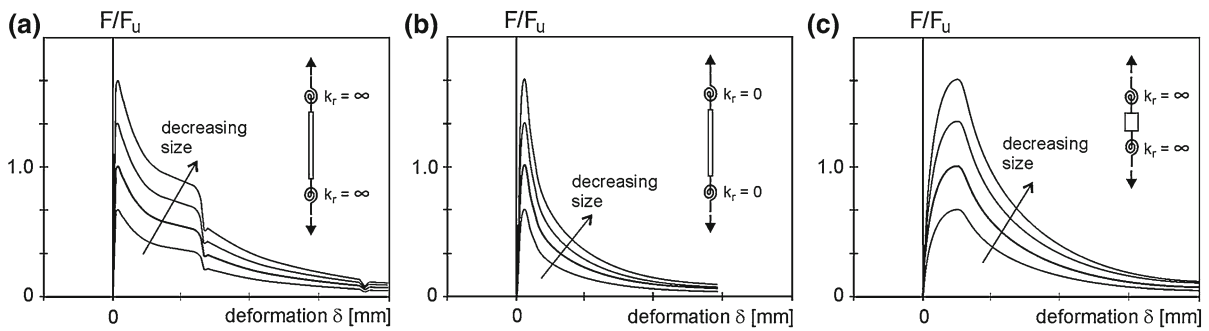

Fig. 2 Effect of boundary rotations on tensile stress-deformation diagram of concrete. In **a** and **b** a slender specimen is loaded between fixed (non-rotating) loading platen and pinned (freely rotating) loading platen, respectively, whereas in **c** fixed specimen ends are used in a test on a stubby specimen

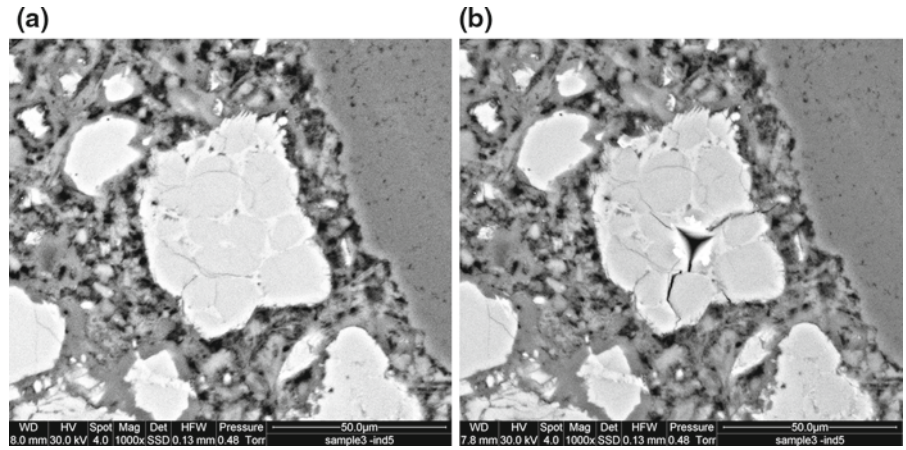

Fig. 3 Two images of a polished surface of hardened cement paste, before (**a**) and after indentation with a Berkovich diamond tip. The almost white particles are the remaining un-hydrated cores of partially hydrated cement grains. *Light gray* and *dark gray* are the low and high-density calcium silicate hydrates (CSH), and *black* is porosity. After Van Mier (2007)

will see how we can still work with such a relationship.

3 Multi-scale modeling?

Recently there has been quite some interest in multi-scale modeling. At the smallest considered size/scale-level the behaviour of the constituents of a composite are determined, for example, and used in sequential analyses at higher size/scale levels, all the way up to the macroscopic (or engineering) level. Does this make sense? It will only work when at the smallest size/scale true material properties are used. In scaling-up to larger size/scale levels boundary effects and size effects can be incorporated, which would lead to correct results at the macroscopic level. The question is thus: are we capable of determining true material properties at the smallest size/scale? In relation to this question immediately a second one can be posed, namely: what is the most appropriate 'smallest' size/scale to start from? Let us assume that we are dealing with concrete and the appropriate lower size/scale-level is the [μm]-level where the structure of hydrated cement can be seen in great detail. In Fig. 3 the structure of cement at the [μm]-size/scale is shown, before and after an indent with a Berkovich diamond tip. The smooth gray area at the right corner of Fig. 3a is part of a sand grain, the more-or-less white particle in the center is an un-hydrated cement grain (approximately 50 μm across), the smaller darker gray patches forming the matrix between the sand and un-hydrated cement particles is hydrated cement, interspersed with porosity, which appears as black specs. The hydrated cement usually comes in two forms: low-density Calcium Silicate Hydrates (in short: CSH) away from the un-hydrated kernel, and high-density CSH directly in contact with the un-hydrated cement grain. In the smallest-scale part of the multi-scale model we need to incorporate all these material phases and, in addition, the interfaces between the various components. A minimum model would require knowledge about the mechanical properties of un-hydrated cement (which is a composite by itself, as can be seen in Fig. 3b after the indentation has been made), low- and high density CSH and at least 3 types of interfaces. The indentation shown in Fig. 3b is one of the few (in-direct) tests available for determining the mechanical properties of these material phases. For instance, Constantinides and Ulm (2004) have attempted to determine the Young's modulus of low- and high-density CSH by means of indentation tests, and reported a higher modulus for high-density CSH in comparison to low-density CSH. Problems in indentation testing are numerous, and just the simple fact that the tests are in-direct makes them suspicious. As an alternative one can try to carry out uniaxial tension tests (see for instance Trtik et al. 2007). Machining tiny specimens of hardened cement paste, or isolating small probes made of the individual cement hydrates (see below) is tedious, and often leads to using larger specimens that contain all the aforementioned material phases. Using a micro-mechanical model one would then have to perform back-calculations and try to estimate the properties of the various material phases. For certain, not a simple task and not a small task either.

An alternative route is to scale-down from the micro-mechanical tensile test and try to obtain specimens consisting of pure cement phases (low-density CSH, high-density CSH, calcium hydroxide and un-hydrated cement), for instance by using a focused ion beam (FIB). This is certainly not an easy task either, but can be done. If we have succeeded in producing the specimens and testing them as well, the same problems that we discussed in the previous Section will return: what to do with size effects and boundary conditions? The answer will not change: again we are measuring structural properties rather than material properties, except perhaps for the Young's modulus and the fracture energy, but these are certainly not sufficient for constructing a fracture model. So, the suggestion to use a lattice model and to feed into the model directly the structural properties of a lattice element might be a workable approach. In the next Section we will explore the advantages and disadvantages of such a model.

4 Structural lattice based on multi-scale interaction potentials (*F-r*)

There is a resemblance between the shape of the attractive part of an atomic potential and the tensile force-deformation diagram for concrete, see Van Mier (2007). A well-known form for the atomic potential for noble gases is the Lennard-Jones (LJ) potential, which may be written as:

$$\frac{V_{LJ}(r)}{\varepsilon} = -4\left[\left(\frac{\sigma}{r}\right)^{12} - \left(\frac{\sigma}{r}\right)^{6}\right], \tag{1}$$

where σ and ε are units of length and energy, respectively. The potential describes the balance between attractive and repulsive forces at the level of atoms. Is the distance between two atoms below the equilibrium separation r_0, the repulsion must be overcome and the atoms must be forced to remain at the prescribed distance. With increasing separation distance between the atoms the energy needed decreases. Equation (1) can be rewritten as:

$$\frac{F}{F_u} = \alpha\left[\left(\frac{\sigma}{r}\right)^{m} - \left(\frac{\sigma}{r}\right)^{n}\right], \tag{2}$$

A relation between the force F to keep the atoms at prescribed separation distance $1/r$. The powers n and m can be varied to obtain the required shape of the potential. In Fig. 4 we show the shape for the parameter

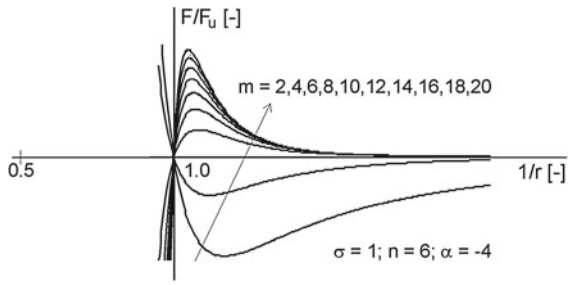

Fig. 4 Variation of the power m in Eq. (2) leads to the family of potentials shown in this Figure. The shape corresponds to the force-deformation diagrams for concrete under uniaxial tension. After Van Mier (2007)

setting $\sigma = 1, n = 6, \alpha = -4$, and m varies between 2 and 20. The curves flip over when $m > 6$. The family of curves above this threshold resembles the shape of a family of force-deformation curves from uniaxial tension tests on concrete, as shown for instance in Fig. 2. It is therefore tempting to investigate whether the simple formulation can be used at higher size/scale-levels as well. Note that the family of curves has been shown relative to the response of a specimen of reference size D_0, having a maximum force F_u.

Beranek and Hobbelman (1992, 1994) showed that a similarity exists between a particle model and a beam lattice model. Starting point was the analysis of a stack of equal-sized spherical particles in contact. The deformations of this model were compared with those of a beam lattice. Lattice beams were assumed to connect the centers of two neighbouring particles. For a certain size of the lattice beams the similarity was perfect, indicating that both models would lead to the same result. The idea is now as follows. A tensile test on a prismatic specimen is interpreted as the potential for a pair of particles of the same size. The so-called pair-potential is thus assumed to apply at larger size/scale levels than the atomic level, even all the way up to the macroscopic size/scale level. Testing a specimen at the required size/scale will yield immediately the required potential. As we show in Fig. 5, we can thus establish the potential at various size/scale-levels such as the nano-, micro-, meso- and macro-levels. Nano would probably be far-fetched when dealing with cement and concrete but the behaviour of the material at the other scales is quite relevant.

Let us now consider the two different interpretations of the meso-structure of concrete as shown in Fig. 6a, b. Following the interpretation of Fig. 6a concrete is seen as a three-phase composite, consisting

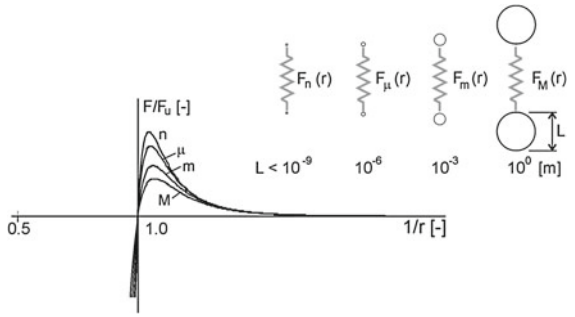

Fig. 5 Pair-potentials for application in a beam-lattice model at various size/scale levels (nano-, micro-, meso- and macro-level). After Van Mier (2012). Note that the potential is active between two particles of identical size; the distance between the particles is here shown exaggerated to indicate that only normal forces are considered between the interacting particles

of cement-matrix in which the various aggregates are embedded. Between the two phases is an interfacial transition zone, which has relatively low strength, and is in fact the weakest part of the concrete structure. Since the matrix is shown here as a continuous phase, we could interpret this visualization as the situation after hydration. The matrix is built up from the smallest sand grains that have not been explicitly included in the model, the Portland cement, and, if present, fly-ash and/or condensed silica. In the lattice model that we built in Delft and Zurich, as a series of consecutive PhD-projects, the visualization of Fig. 6a was taken as a starting point. The regular or random lattice was simply projected on top of the 3-phase material structure and properties were assigned depending on where a certain lattice element would be located, see Fig. 6c. In Fig. 6b concrete is depicted as a stack of spherical particles of varying size. In a way this is the situation before the cement hydrates; only the water needed for hydration is not shown in this Figure (note that the mixing water in concrete is initially absorbed at the particle's surfaces and possible excess water will gather in voids between the particles). All particles sizes are present: from the largest [mm]-size aggregates to the smallest (sub-[μm] size) fly-ash and condensed silica particles with the cement grains of a size falling between these extremes. With such a hierarchical system the densest possible material structure can be obtained, which will have the highest possible strength. The material interpretation of Fig. 6b can also be turned into a lattice. By simply connecting the centers of neighbouring particles a lattice is constructed. Each lattice element represents the interaction between the two neighbouring particles. Interpreting the system as just a bunch of pair-interactions is probably too simple, and higher order interactions may be included, at the cost of a loss in transparency of the model. In Fig. 6d the connectivity between the particle centers is shown, in Fig. 6e the remaining lattice.

The potential law, Eq. (2) describes the behaviour of a lattice element, but an essential adjustment must be made. The potential used in our lattice model depends on the actual size of the individual lattice elements, and on the rotational support stiffness at both nodes, i.e. the connectivity to the other lattice elements. The rotational stiffness at the supports depends not only on the connectivity to the rest of the lattice but also on the flexural stiffness of the lattice element itself. So, rather than descending to a so-called material level, and describing the properties of the lattice elements via constitutive equations, we remain at the 'structural level' and describe the properties of each lattice element directly as a function of size and support conditions. The complication that arises in conventional cohesive fracture models is solved, namely the dependence of cohesive fracture properties on element size and boundary conditions is now implicitly included in the model. Figure 7 shows examples of (size-dependent) potentials for three different boundary conditions and varying specimen slenderness. Specific characteristics of a lattice element are included in the $F - r$ potential. For instance the 'bump' in the softening curve when a slender lattice element is tested between fixed boundaries is included in the potential function. It is not seen as an 'inconvenience' that at all costs must be removed from the model. No, it is just part of the behaviour of that particular lattice element when the element's ends are fixed against rotations. Likewise we will have to use the smooth curve for a lattice element between pinned supports, which is actually a condition that will not be found in a beam lattice model, and the increased pre-peak deformations for a stubby lattice beam between fixed supports. The latter case may appear frequently since in the beam lattices explored to date always relatively stubby elements have been used, which came from the demand to justify the elastic lattice properties to those of a real concrete specimen or structure; see for instance in Schlangen and Mier (1994).

Returning to the model of Fig. 6d, e, which was derived from the concrete material structure of Fig. 6b,

we can easily see the implications of this model. For compression the effects from bc on lattice element response are even more pronounced in comparison to the effects shown here for tension; see the overview in Chapter 8 in Van Mier (2012). The same approach as sketched above can be applied, however. As an example consider the particle stack of equal-sized disks (2D is considered for explaining the matter here) subjected to external compression in Fig. 8a. The contact forces between the particles are either compressive or tensile (splitting forces will occur between horizontal oriented particle pairs), as shown in the equivalent lattice model. If the disks are of varying size the lattice element sizes vary correspondingly and the potential functions describing the relation between lattice element force F and deformation r will vary as well.

5 Which experiments are essential?

In the model approach suggested in the previous section the behaviour of a lattice element is described directly in terms of force and deformation. The consequence is that for each lattice element size and bc the behaviour must be estimated from experiments. How can this be done? In the first place the task will be simplified by considering a limited set of bc's, which could be identified from elastic analyses of a corresponding beam lattice. The size of the lattice elements can be set using the approach in Schlangen and Mier (1994). After the rotational stiffnesses of the two nodes of an element have been established, we know how large the specimen should be as well as the rotational support stiffnesses. After that it is rather simple and straightforward to conduct the experiment. The main advantage of the

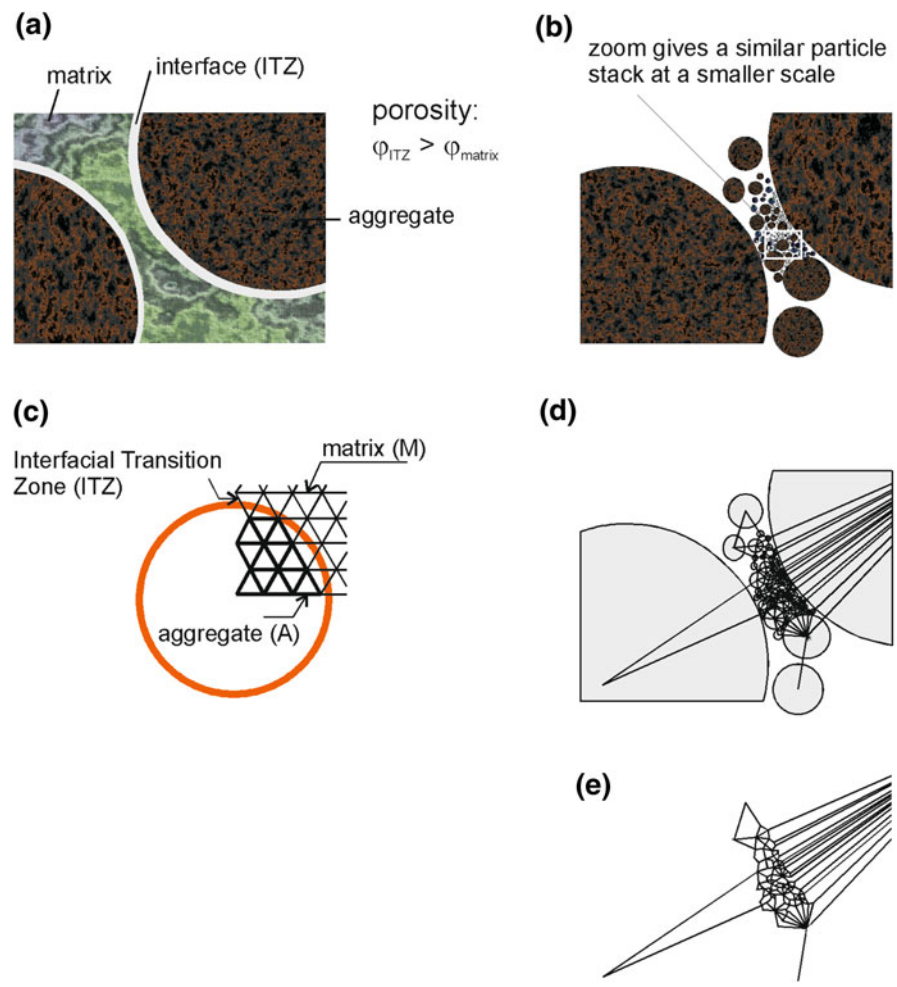

Fig. 6 Two different interpretations of the meso-structure of concrete: **a** concrete as a three-phase composite of matrix, aggregate and interfacial transition zone (ITZ), and **b** as a stack of particles of different size. The model of (**a**) has been used frequently in the past: a regular or random lattice was projected on top of the material structure and the lattice elements would be assigned properties according their location on the material structure as shown in (**c**). In the model of (**b**) particles can be anything from gravel, sand, condensed silica, Portland cement, fly-ash, and so on. The particle stack of (**b**) can form the basis for the construction of a lattice as shown in (**d**) and (**e**), which would form the basis of the 'structural lattice' discussed in this paper

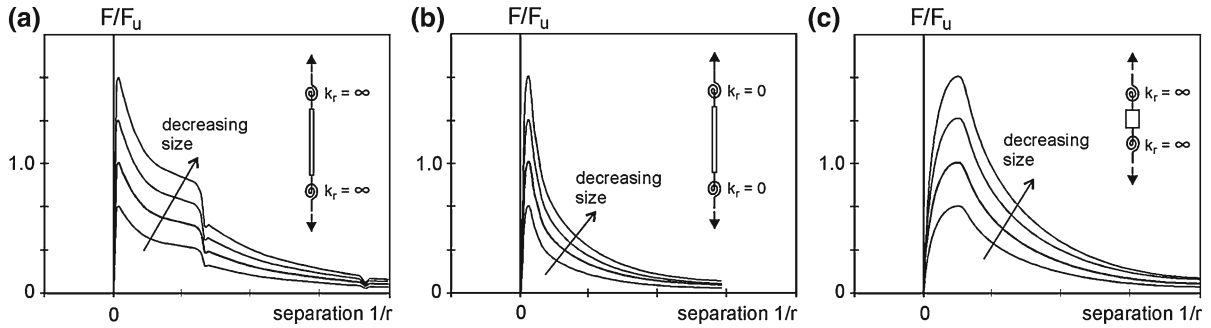

Fig. 7 Examples of pair-potentials $F/F_u - r$ for three different structural conditions of the lattice element: **a** slender lattice element loaded between fixed (no-rotating) ends, **b** slender lattice element loaded between pinned ends, and **c** stubby lattice element between fixed ends

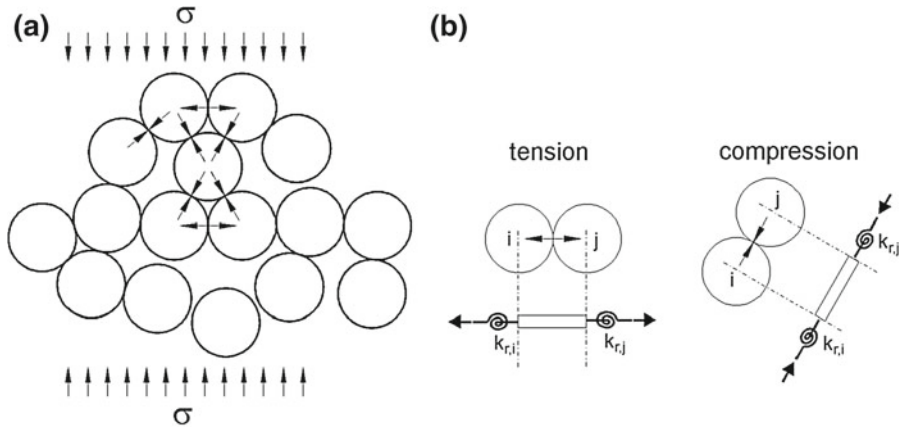

Fig. 8 Stack of equal-sized disks subjected to external compression (**a**). Tensile splitting forces develop between horizontal pairs and compressive stresses are transmitted between vertically arranged particle pairs or inclined pairs. In (**b**) the equivalent lattice element and its boundary conditions are shown. The input potential is simply what is measured for such a lattice element in a physical experiment

procedure sketched here is that the basis of the model approach is defined from the constraints set by laboratory experiments. The model is defined based on what we can actual derive from physical experiments and no ad-hoc assumptions are necessary. As we have discussed in Sect. 2 properties for cohesive crack models are dependent on specimen size and bc, and in that respect cohesive crack models are rather useless. The situation is more severe for compression than for tension. With the new approach one could argue that many different specimen sizes and bc's must be tested. Indeed this is the case, but probably the number of cases can be reduced significantly by simplifying the material structure to some extent, for instance leaving out all particles below a certain size-threshold. Such simplifications were also made in the lattice model mentioned before (Schlangen and Van Mier 1992 and Lilliu and Van Mier 2003), but the model outcomes will still be useful for obtaining a profoundly improved insight in the fracture behaviour of cement and concrete. Unfortunately the simplicity and transparency of the original lattice model are lost to some extent. Yet, the fit of the load-displacement curve should improve substantially. Since any type of structure is calculated as such (i.e. reconstructing the exact boundary conditions), there is no need to assume that some properties are 'material properties'. We simply calculate the effects from structure size and boundary conditions and the effort will be rewarded because the model starts from the behaviour of single lattice elements that can actually be measured in laboratory experiments. In principle the fictitious crack model also predicts size effects; yet there

an un-resolved problem remains, i.e. softening is not a material property.

Next to the tests aimed at establishing the potential-law for the individual lattice elements, large scale tests on larger material volumes are quite essential, in particular the determination of the evolution of the crack populations under a variety of loading paths. These large-scale tests are needed to establish fracture mechanisms. A useful approach is the use of X-ray tomography, which can provide the evolution of the full three-dimensional crack population in time; see for instance Trtik et al. (2007) and Meyer et al. (2009).

6 Conclusion

In this paper we discuss an alternative to cohesive crack models, namely a lattice model based on $F - r$ potentials. The potential function to be used depends on the size of the lattice element (slenderness h/d) and the rotational stiffness at the nodes. The rotational stiffness at the nodes of each lattice element depends on the connectivity of an element to neighbouring lattice elements as well as on the flexural stiffness of the lattice elements themselves. The implication is that for a variety of boundary conditions and a variety of lattice element sizes the potential function must be measured, but the enormous advantage is that what is needed as input in the model can actually be measured in physical experiments. The potential describes the structural behaviour of a lattice element. Material properties do not exist, which is the main deviation here from assumptions in cohesive models where the softening curve is considered as a material property. Basically we start from what can be measured in a fracture experiment, in stead of trying to measure haphazardly proposed parameters. The model approach explained in this short paper is an elegant manner to overcome the parameter-identification conundrum which seems to affect most fracture models today.

References

Akita H, Koide H, Mihashi H (2007) Specimen geometry in uniaxial tension test of concrete. In: Carpinteri A et al (eds) Proceedings FraMCoS-6. Taylor & Francis, London, pp 243–248

Bažant ZP (1984) Size effect in blunt fracture: concrete, rock, metal. J Eng Mech 110:518–535

Beranek WJ, Hobbelman GJ (1992) Handboek voor het mechanisch gedrag van metselwerk (Glossary of the mechanical behaviour of masonry). Report C-77, CUR Foundation, Gouda (in Dutch)

Beranek WJ, Hobbelman GJ (1994) Constitutive modelling of structural concrete as an assemblage of spheres. In: Mang H, Bicanic N, de Borst R (eds) Computational models of concrete structures, proceedings EURO-C. Pineridge Press, Swansea, pp 535–542

Carpinteri A, Chiaia B, Cornetti P (2003) On the mechanics of quasi-brittle materials with a fractal microstructure. Eng Fract Mech 70:2321–2349

Constantinides G, Ulm FJ (2004) The effect of two types of C-S-H on the elasticity of cement-based materials: results from nano-indentation and micro-mechanical modeling. Cem Conc Res 34(1):67–70

Duan K, Hu X (2004) Specimen boundary induced size effect on quasi-brittle fracture. Strength Fract Complex 2:47–68

Evans RH, Marathe MS (1968) Microcracking and stress-strain curves for concrete in tension. Mater Struct (RILEM) 1(1):61–64

Herrmann HJ, Hansen A, Roux S (1989) Fracture of disordered elastic lattices in two dimensions. Phys Rev B 39(1): 637–648

Hillerborg A, Modeér M, Peterson P-E (1976) Analysis of crack formation and crack growth in concrete by means of fracture mechanics and finite elements. Cem Conc Res 6:773–782

Hordijk DA (1991) Local approach to fatigue of concrete. PhD thesis, Delft University of Technology

Ince R, Arslan A, Karihaloo BL (2003) Lattice modeling of size effect in concrete strength. Eng Fract Mech 70:2307–2320

Lilliu G, Van Mier JGM (2003) 3D lattice type fracture model for concrete. Eng Fract Mech 70(7/8):927–942

Meyer D, Man H-K, Van Mier JGM (2009) Fracture of foamed cementitious materials: a combined experimental and numerical study. In: Zhao H, Fleck NA (eds), Mechanical properties of cellular materials. New York: IUTAM Bookseries 12, Springer Science+ Business, Media, 115–123

Mindess S (1991) Fracture process zone detection. In: Shah SP, Carpinteri A (eds) Fracture mechanics test methods for concrete. Chapman & Hall, London, pp 231–261

Roux S, Guyon E (1985) Mechanical percolation: a small beam lattice study. J Phys Lett 46:L999–L1004

Schlangen E, Van Mier JGM (1992) Experimental and numerical analysis of the micro-mechanisms of fracture of cement-based composites. Cem Conc Comp 14(2):105–118

Schlangen E, Van Mier JGM (1994) Fracture simulations in concrete and rock using a random lattice. In: Siriwardane H, Zaman MM (eds) Computer methods and advances in geomechanics. Balkema, Rotterdam, pp 1641–1646

Termonia Y, Meakin P (1986) Formation of fractal cracks in a kinetic fracture model. Nature 320:429–431

Trtik P, Stähli P, Landis EN, Stampanoni M, Van Mier JGM (2007) Microtensile testing and 3D imaging of hydrated portland cement. In: Carpinteri A, Gambarova P, Ferro G, Plizzari G (eds), Proceedings 6th international conference on fracture mechanics of concrete and concrete structures (FraMCoS-VI). London: Taylor & Francis, 1277–1282

Van Mier JGM (1986) Fracture of concrete under complex stress. HERON 31(3):1–90

Van Mier JGM (2007) Multi-scale interaction potentials ($F - r$) for describing fracture of brittle disordered materials like cement and concrete. Int J Fract 143(1):41–78

Van Mier JGM (2009) Mode II fracture localization in concrete loaded in compression. J Eng Mech (ASCE) 135(1):1–8
Van Mier JGM (2012) Concrete fracture—multiscale approach. Taylor & Francis/CRC Press, Boca Raton
Van Mier JGM, Nooru-Mohamed MB (1990) Geometrical and structural aspects of concrete fracture. Eng Fract Mech 35(4/5):617–628
Van Mier JGM, Schlangen E, Vervuurt A (1995) Lattice type fracture models for concrete. In: Mühlhaus H-B (ed) Continuum models for materials with micro-structure. Wiley, Chichester, pp 341–377
Van Mier JGM, Shi C (2002) Stability issues in uniaxial tensile tests on brittle disordered materials. Int J Solids Struct 39:3359–3372
Van Mier JGM, Van Vliet MRA (2003) Influence of microstructure of concrete on size/scale effects in tensile fracture. Eng Fract Mech 70(16):2281–2306
Van Vliet MRA, Van Mier JGM (2000) Experimental investigation of size effect in concrete and sandstone under uniaxial tension. Eng Fract Mech 65(2/3):165–188
Weibull W (1939) A statistical theory of strength of materials. Roy Swedish Inst Eng Res 151:1–45